INHIBITION OF CONFINED HYDROGEN EXPLOSION BY INERT GASES

Li, Y.[1], Bi, M.[1], Ren, J.[1], Gan, B.[1], Yan, C.[1], Gao, W.[1]
[1] College of Chemical Engineering, Dalian University of Technology, Dalian, 116024, China

ABSTRACT

This paper is aimed at revealing the inhibiting effects of He, Ar, N_2 and CO_2 on confined hydrogen explosion. The flame characteristics under thermodiffusive instability and hydrodynamic instability are analyzed using Lewis number and ratio of density ratio to flame thickness. The inhibiting effects of inert gas on confined hydrogen explosion are evaluated using maximum explosion pressure and maximum pressure rise rate. The inhibiting mechanism is obtained by revealing thermal diffusivity, maximum mole fraction and net reaction rate of active radicals. The results demonstrated that the strongest destabilization effect of hydrodynamic instability and thermodiffusive instability occurs when the inert gas is Ar and CO_2, respectively. Taking maximum explosion pressure and maximum rate of pressure rise as an indicator, the effects of confined hydrogen explosion inhibition from strong to weak are CO_2, N_2, Ar and He. Laminar burning velocity, thermal diffusivity, maximum mole fraction and net reaction rate of active radicals, continues to decrease in the order of He, Ar, N_2 and CO_2. The elementary reactions of generating and consuming active radicals at the highest net reaction rate are mainly consisted of R1 ($H+O_2=OH+O$), R2 ($H_2+O=OH+H$), R3 ($H_2+OH=H_2O+H$) and R10 ($HO_2+H=2OH$).

Nomenclature

c_p	specific heat, J/kg/K
D_T	thermal diffusivity, m2/s
D_{iM}	mass diffusivity, m2/s
Le	Lewis number
$n_{hydrogen}$	mole number of hydrogen, mole
n_{inert}	mole number of inert gas, mole
n_{oxygen}	mole number of oxygen, mole
S_L	laminar burning velocity, m/s
T_{ad}	adiabatic flame temperature, K
T_0	initial temperature, K
δ	flame thickness, mm
λ	thermal conductivity, J/m/K/s
ρ_u	unburnt mixture density, kg/m3
ρ_b	burnt product density, kg/m3
σ	density ratio

1.0 INTRODUCTION

As an environment-friendly fuel, hydrogen energy is generated in large quantities to supply power throughout the world. But the extremely dangerous explosion properties also limit the wide application of hydrogen energy from the safety perspective. Especially when the thermodiffusive instability and hydrodynamic instability are emerged, the hydrogen flame morphologies will undergo the transition from smooth flame to cellular flame, this will enhance explosion pressure and result in personnel injuries and property losses [1-3]. Therefore it is in urgent need to suppress or mitigate hydrogen explosion in developing hydrogen economy.

Up to now, some works have been performed to mitigate the hydrogen explosion intensity. Azatyan et al. [4] numerically studied the influence of N_2, CO_2 and steam on laminar burning velocity of hydrogen-air mixture and found that the laminar burning velocity decreases gradually with an increase in the additive content. Pang et al. [5] experimentally investigated the deflagration characteristics of hydrogen-air mixture inside a mesh aluminum alloys-filled tube. The results indicated that the mesh aluminum alloy is unstable to suppress the hydrogen-air deflagration, which could increase maximum

explosion pressure. Cheikhravat et al. [6] revealed the interaction between droplets and hydrogen-air-steam flame propagation and pointed out that the non-flammable mixture at 358K and 383K could be made explosive by aspersion with cold water spray. Especially when the droplets diameter is less than 10μm, the explosion intensity could be suppressed except for the lean mixture. Ingram et al. [7-8] concluded that as the fine water mist increases, the burning velocity of H_2-O_2-N_2 could be reduced significantly and the flame instabilities will enhance substantially. Especially when the NaOH is added into the water mist, the range of flammable compositions could be reduced considerably. Sikes et al. [9] obtained the laminar flame speeds of DEMP (diethyl methylphosphonate), DMMP (dimethyl methylphosphonate) and TEP (trimethyl phosphate) added to hydrogen-air mixtures and found that an increasing suppression effect corresponds to a higher carbon moiety.

In summary, the hydrogen explosion mitigation is focused on obtaining laminar burning velocity and flammable range. The flame characteristics and explosion pressure under He, Ar, N_2 and CO_2 atmosphere are compared rarely. In view of this, this paper firstly reveals the effect of inert gas on flame morphologies, maximum explosion pressure and maximum pressure rise rate. Then inhibition mechanism of inert gas on confined hydrogen explosion is obtained by analysing thermal diffusivity, maximum mole fraction and net reaction rate of active radicals.

2.0 EXPERIMENTAL APPARATUS

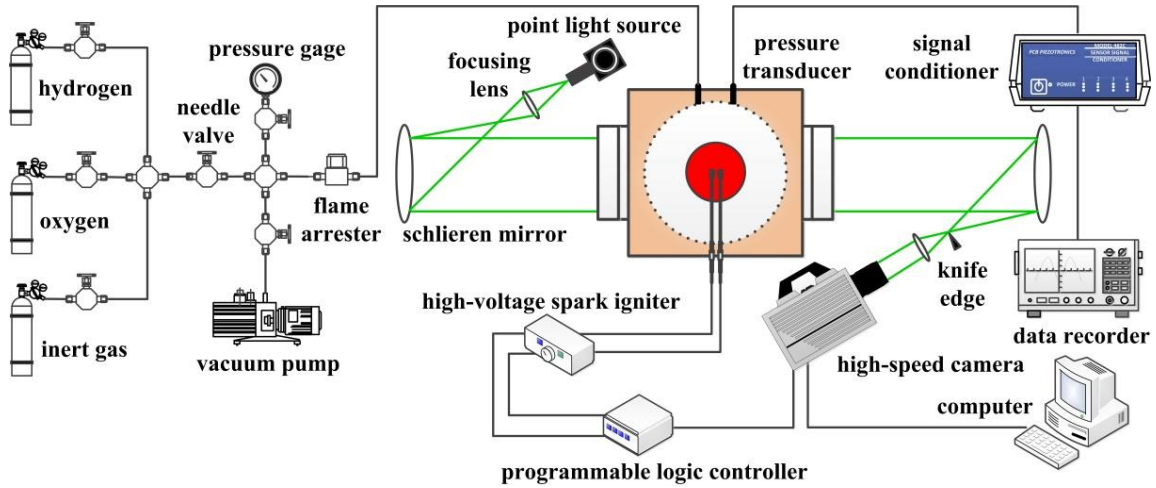

Fig.1 Schematic of experimental apparatus

The experimental apparatus has been presented in our previous works [10-11], which is consisted of a spherical combustion chamber, a high-speed schlieren system, a pressure measurement system, a high-voltage spark igniter, a data recorder and a programmable logic controller. After evacuation, the hydrogen, inert gas and oxygen are fed into the combustion chamber. The composition of combustible mixture is obtained using the method of partial pressure. Before ignition, about five minutes is needed to ensure combustible mixture quiescent. As shown in Fig.1, through the visualization window with the diameter of 120mm, the flame morphology is filmed using high-speed schlieren system at the shoot speed of 10000frame/s. The transient pressure is measured using PCB piezotronics pressure transducer (113B24) and is recorded using YOKOGAWA data recorder with the sampling rate of 100kS/s. In order to evaluate the inhibition effect of inert gas on confined hydrogen explosion, He, Ar, N_2 and CO_2 are adopted in this work and the volume ratio of inert gas to oxygen still remains to be 3.76. The equivalence ratio (Φ=0.8, Φ=1.0 and Φ=1.5) is adopted in the experiment and the equivalence ratio is defined as follows:

$$\Phi = \frac{\dfrac{n_{hydrogen}}{n_{inert}+n_{oxygen}}}{\left(\dfrac{n_{hydrogen}}{n_{inert}+n_{oxygen}}\right)_{st}} \tag{1}$$

3.0 RESULTS AND DISCUSSIONS

3.1 Flame morphologies under inert gas atmosphere

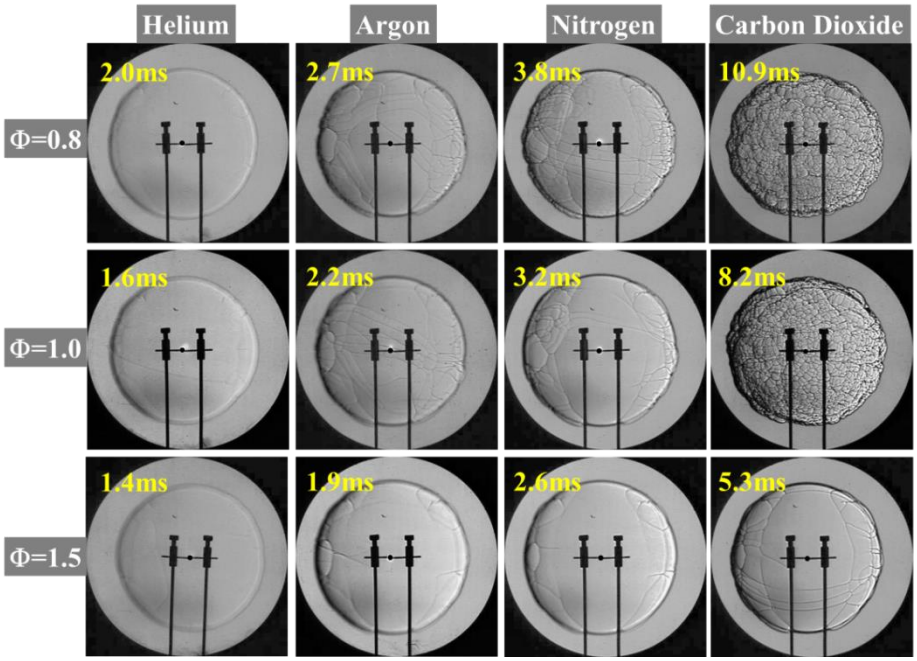

Fig.2 Flame morphologies under He, Ar, N_2 and CO_2 atmosphere

According to the published works [12-13], it is well known that the flame instabilities should increase flame surface area and hence enhance explosion pressure. Therefore, the effects of thermodiffusive instability and hydrodynamic instability on flame morphologies under He, Ar, N_2 and CO_2 atmosphere are firstly presented in Fig.2. Under He atmosphere, the expanding flame presents a smooth structure at Φ=0.8, Φ=1.0 and Φ=1.5. The crack flame could be observed under Ar and N_2 atmosphere, and the crack number on the lean and stoichiometric side is more than that on the rich side. Under CO_2 atmosphere, the cellular flame is only formed at Φ=0.8 and Φ=1.0. In addition, for a given equivalence ratio, the decreasing order of flame propagation velocity is: He, Ar, N_2 and CO_2.

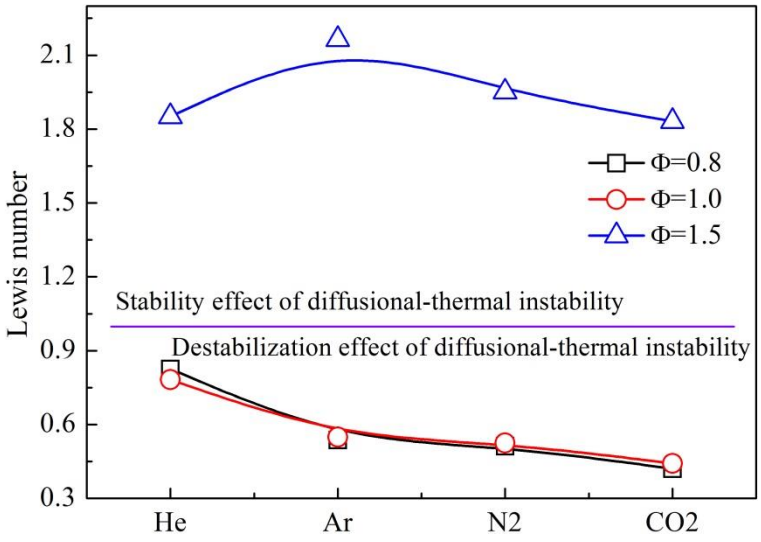

Fig.3 Lewis number under He, Ar, N_2 and CO_2 atmosphere

Due to the unequal diffusion of mass and heat inside flame front, the thermodiffusive instability occurs, which could be characterized by Lewis number. Under thermodiffusive instability, the outwardly propagating flame tends to be unstable and stable when $Le<1.0$ and $Le>1.0$, respectively. When the

Lewis number is equal to one, the outwardly propagating flame is only affected by hydrodynamic instability. As an intrinsic instability, the hydrodynamic instability results from the density disparity between unburnt mixture and burnt product, which is characterized by density ratio and flame thickness. In order to reveal flame characteristics under thermodiffusive instability and hydrodynamic instability, the Lewis number, density ratio and flame thickness are calculated as follows [14-16]:

$$Le = \frac{D_T}{D_{iM}} \tag{2}$$

$$\sigma = \frac{\rho_u}{\rho_b} \tag{3}$$

$$\delta = \frac{2\lambda}{\rho_u c_p S_L}\left(\frac{T_{ad}}{T_0}\right)^{0.7} \tag{4}$$

Fig.3 shows the Lewis number under He, Ar, N_2 and CO_2 atmosphere. When the equivalence ratio is Φ=1.5, the Lewis number is still larger than one under He, Ar, N_2 and CO_2 atmosphere, which indicates that the thermodiffusive instability could stabilize the hydrogen flame. When the equivalence ratio is Φ=0.8 and Φ=1.0, the Lewis number is less than one and the Lewis number continues to decrease in the following order: He, Ar, N_2 and CO_2, which indicates that the lean and stoichiometric flame tends to be unstable under thermodiffusive instability.

Considering the fact that the density ratio is the most fundamental factor of controlling hydrodynamic instability and the thinner flame could result in a stronger destabilizing propensity [17]. In order to quantify the effect of hydrodynamic instability on flame destabilization more intuitively, the ratio of density ratio to flame thickness under He, Ar, N_2 and CO_2 atmosphere is given in Fig.4. By varying equivalence ratio, it is found that the ratio of density ratio to flame thickness reaches the peak value under Ar atmosphere and reaches the minimum value under CO_2 atmosphere. The above results also indicate that the destabilization effect of hydrodynamic instability is strongest under Ar atmosphere and is weakest under CO_2 atmosphere.

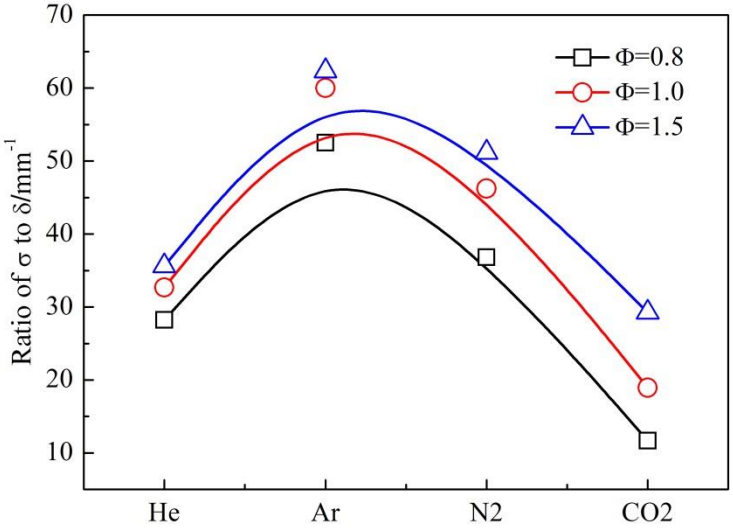

Fig.4 Ratio of density ratio to flame thickness under He, Ar, N_2 and CO_2 atmosphere

Theoretically, under thermodiffusive instability, the strongest destabilization effect occurs under CO_2 atmosphere when the equivalence ratio is Φ=0.8. Under hydrodynamic instability, the strongest destabilization effect occurs under Ar atmosphere when the equivalence ratio is Φ=1.5. In combination with Fig.2, the condition corresponding to strongest level of flame destabilization is: Φ=0.8 and under CO_2 atmosphere, which also means that at normal temperature and normal pressure, the main factor of affecting flame destabilization is thermodiffusive instability.

3.2 Maximum explosion pressure and maximum rate of pressure rise

In order to compare the inhibiting effect of inert gas on confined hydrogen explosion, the maximum

explosion pressure and maximum pressure rise rate are regarded as evaluation parameters. Fig.5 gives the maximum explosion pressure and maximum pressure rise rate under He, Ar, N_2 and CO_2 atmosphere. For a given equivalence ratio, both maximum explosion pressure and maximum pressure rise rate continue to decrease in the order of He, Ar, N_2 and CO_2. Comparing maximum explosion pressure and maximum pressure rise rate under He and CO_2 atmosphere, the maximum reduction of maximum explosion pressure and maximum pressure rise rate is as high as 57.1% and 94.7% (Φ=0.8), respectively. The above results also demonstrate that the inhibition of CO_2 on hydrogen explosion is much higher than that of the other inert gases.

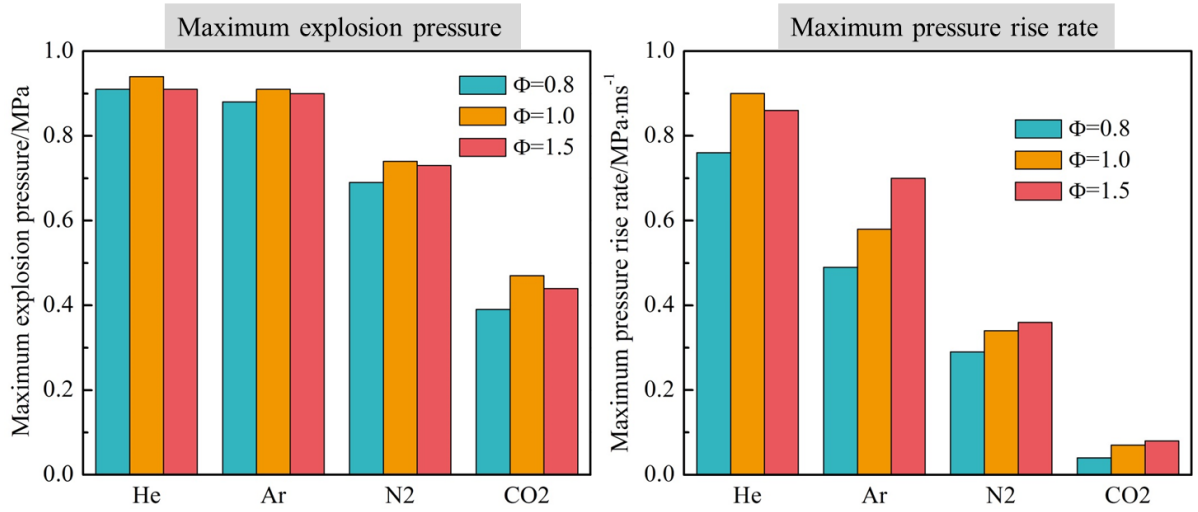

Fig.5 Maximum explosion pressure and maximum pressure rise rate under He, Ar, N_2 and CO_2 atmosphere

3.3 Inhibition mechanism of inert gases

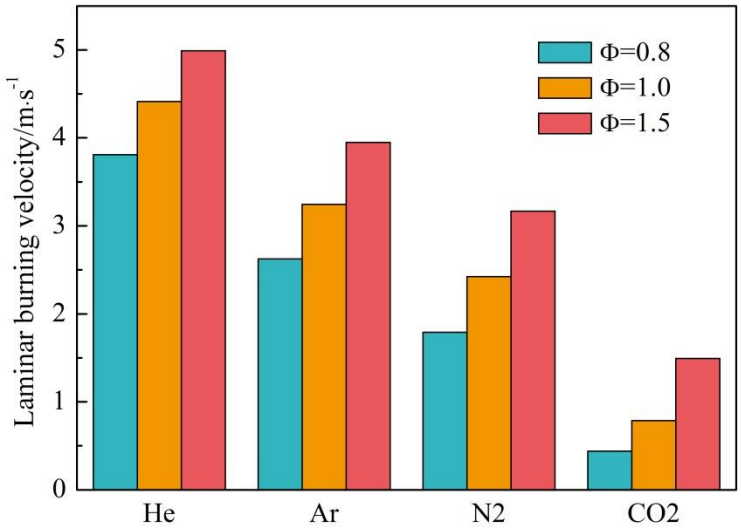

Fig.6 Laminar burning velocity under He, Ar, N_2 and CO_2 atmosphere

According to the published works [10-11], the confined explosion pressure behavior is strongly related to laminar burning velocity when the flame instabilities are neglected. In order to obtain the inhibition mechanism of inert gas on confined hydrogen explosion, the laminar burning velocity and the corresponding controlling factors (such as thermal diffusivity, laminar flame structure, maximum mole fraction and net reaction rate of active radicals) are obtained using PREMIX code and GASEQ. Note that the San Diego Mechanism [18] is coupled in the PREMIX code. Fig.6 gives the laminar burning velocity under He, Ar, N_2 and CO_2 atmosphere. For a given inert gas, the laminar burning velocity increases gradually from Φ=0.8 to Φ=1.5. When the equivalence ratio is fixed, the decreasing order of laminar burning velocity is: He, Ar, N_2 and CO_2.

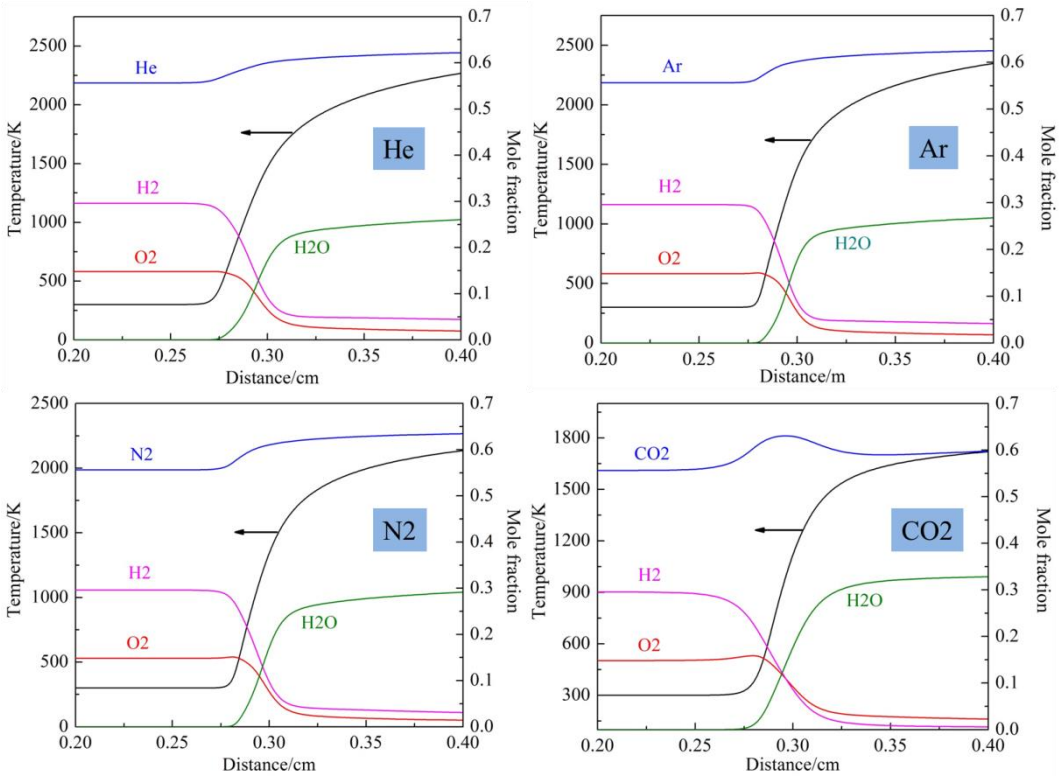

Fig.7 Laminar flame structure under He, Ar, N_2 and CO_2 atmosphere (Φ=1.0)

In fact, the laminar burning velocity, positively correlated with the concentration of active radicals, is proportional to square root of multiplication of thermal diffusivity and chemical reaction rate [19-21]. Before analysing thermal diffusivity, maximum mole fraction and net reaction rate of active radicals, the laminar flame structure under He, Ar, N_2 and CO_2 atmosphere is firstly given in Fig.7. Due to the fact that H_2O is generated through the combustion reaction of hydrogen and oxygen, the mole fraction of H_2 and O_2 in unburnt mixture is significantly larger than that in burnt product, the mole fraction of H_2O and temperature increase monotonously accompanied with the transition from unburnt mixture to burnt product. Under He, Ar and N_2 atmosphere, the mole fraction of inert gas increase gradually through flame front. But under CO_2 atmosphere, the mole fraction of CO_2 increases firstly and then decrease through flame front. Especially under He and Ar atmosphere, the reacting temperature is almost equal, which also indicates that the reacting temperature is not the main factor of affecting laminar burning velocity under He and Ar atmosphere.

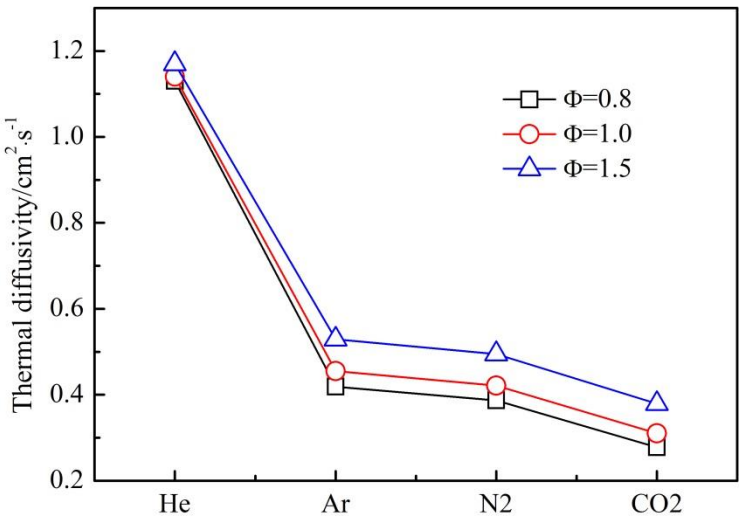

Fig.8 Thermal diffusivity under He, Ar, N_2 and CO_2 atmosphere

Fig.8 shows the thermal diffusivity under He, Ar, N_2 and CO_2 atmosphere. There is extremely similar tendency between laminar burning velocity and thermal diffusivity. For a given inert gas, the decreasing order of thermal diffusivity is: Φ=1.5, Φ=1.0 and Φ=0.8. And the thermal diffusivity of various equivalence ratios continues to decrease in the order of He, Ar, N_2 and CO_2. Fig.9 shows the maximum mole fraction of active radicals (H, OH and O) under He, Ar, N_2 and CO_2 atmosphere. For a given inert gas, the decreasing order of maximum mole fraction of active radicals is: H, OH and O. The decreasing order of maximum mole fraction of active radicals is: He, Ar, N_2 and CO_2, which tendency is consistent with that of laminar burning velocity. Actually, the reduction of thermal diffusivity and maximum mole faction of active radicals contributes to the decrease of laminar burning velocity.

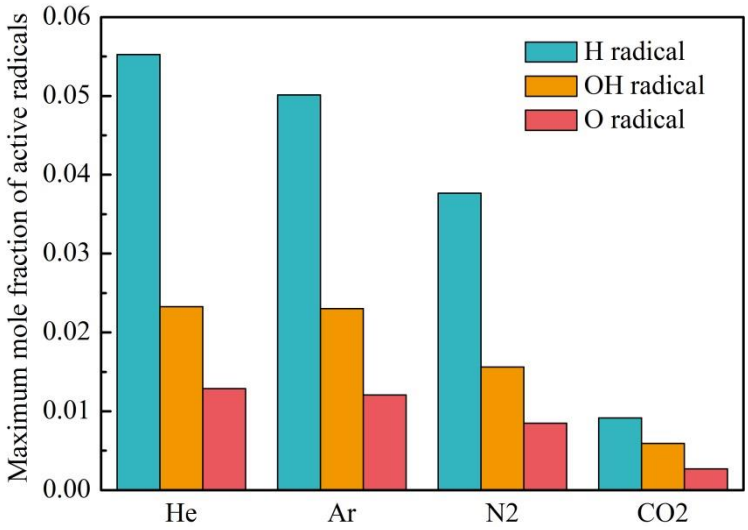

Fig.9 Maximum mole fraction of active radicals under He, Ar, N_2 and CO_2 atmosphere (Φ=1.0)

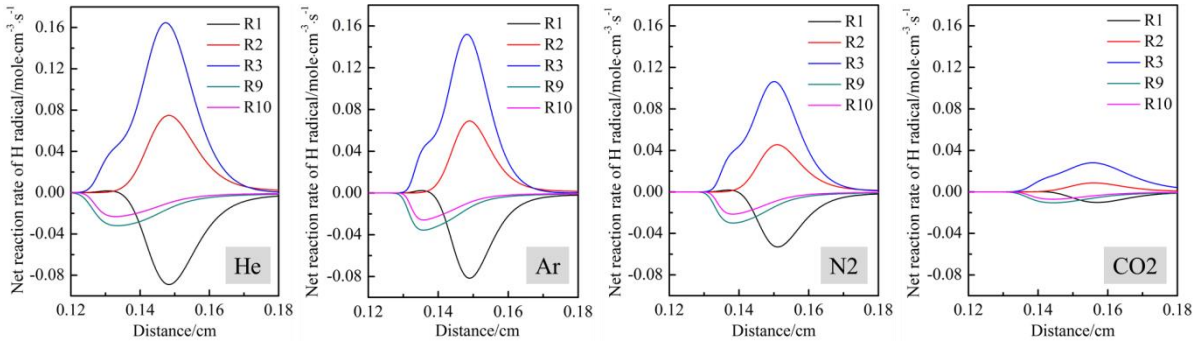

Fig.10 Net reaction rate of H radical under He, Ar, N_2 and CO_2 atmosphere (Φ=1.0)

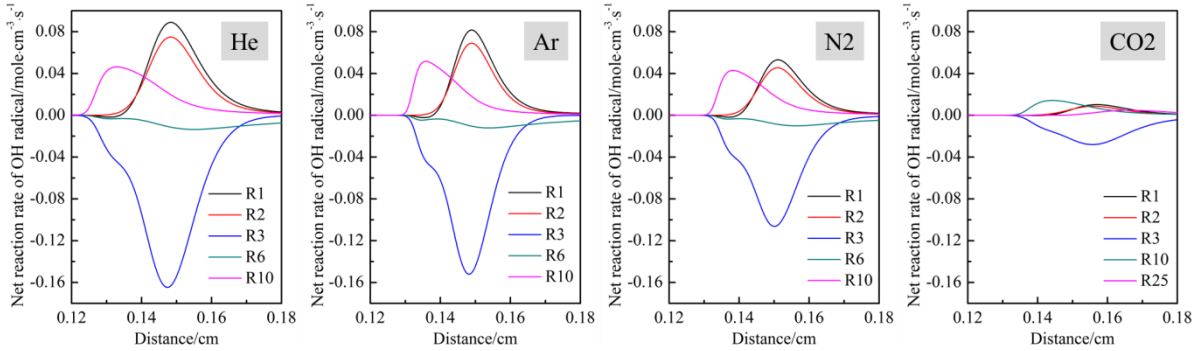

Fig.11 Net reaction rate of OH radical under He, Ar, N_2 and CO_2 atmosphere (Φ=1.0)

In order to evaluate the contributions of elementary reaction to maximum mole fraction of active radicals, the net reaction rate of H, OH and O radicals under He, Ar, N_2 and CO_2 atmosphere is shown

in Fig.10-12. The reaction step and elementary reaction is listed in Table.1. Obviously, the net reaction rate of generating and consuming active radicals continues to decrease in the order of He, Ar, N_2 and CO_2. The elementary reaction of generating and consuming H radical at the highest net reaction rate is R3 (H_2+OH=H_2O+H) and R1 (H+O_2=OH+O), respectively. Under various inert gases atmosphere, the elementary reaction of consuming OH radical at the highest rate is still R3 (H_2+OH=H_2O+H). Under He, Ar and N_2 atmosphere, R1 (H+O_2=OH+O) has the highest net reaction rate of generating OH radical, and R10 (HO_2+H=2OH) does under CO_2 atmosphere. The R1 (H+O_2=OH+O) and R2 (H_2+O=OH+H) has a highest net reaction rate of generating and consuming O radical under various inert gases atmosphere.

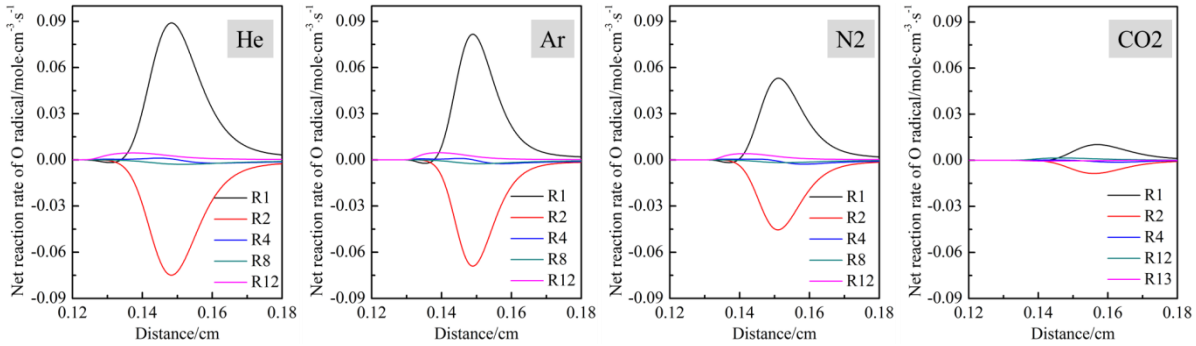

Fig.12 Net reaction rate of O radical under He, Ar, N_2 and CO_2 atmosphere (Φ=1.0)

Table.1 Step number and elementary reaction

Reaction Step	Elementary reaction
R1	H+O_2=OH+O
R2	H_2+O=OH+H
R3	H_2+OH=H_2O+H
R4	H_2O+O=2OH
R6	H+OH+M=H_2O+M
R8	H+O+M=OH+M
R9	H+O_2(+M)=HO_2(+M)
R10	HO_2+H=2OH
R12	HO_2+H=H_2O+O
R13	HO_2+O=OH+O_2
R25	CO+OH=CO_2+H

4.0 CONCLUSIONS

In this work, the flame characteristics and explosion pressure under He, Ar, N_2 and CO_2 atmosphere are experimentally obtained using high-speed schlieren system and pressure measurement system, respectively. Firstly, the effects of thermodiffusive instability and hydrodynamic instability on flame destabilization are revealed. Then the confined hydrogen explosion inhibition is evaluated using maximum explosion pressure and maximum pressure rise rate. Finally, the inhibitive mechanism of inert gas is analyzed using thermal diffusivity, maximum mole fraction and net reaction rate of active radicals. The main conclusions are as follows:

(1) The strongest destabilization effect of hydrodynamic instability and thermodiffusive instability occurs when the inert gas is Ar and CO_2, respectively. By varying equivalence ratio, the main factor of controlling flame destabilization is thermodiffusive instability under various inert gases atmosphere.

(2) Both maximum explosion pressure and maximum pressure rise rate continue to decrease in the order of He, Ar, N_2 and CO_2. Under He and CO_2 atmosphere, the maximum reduction of maximum explosion pressure and maximum pressure rise rate is as high as 57.1% and 94.7% (Φ=0.8), which means that CO_2 is the best suited to inhibit confined hydrogen explosion under various inert gases atmosphere.

(3) Laminar burning velocity, thermal diffusivity, maximum mole fraction and net reaction rate of

active radicals, continue to decrease in the order of He, Ar, N_2 and CO_2, which contributes to the reduction of maximum explosion pressure and maximum pressure rise rate.

(4) Under He, Ar, N_2 and CO_2 atmosphere, the elementary reactions of generating H, OH and O radicals at the highest net reaction rate include R1 ($H+O_2=OH+O$), R3 ($H_2+OH=H_2O+H$) and R10 ($HO_2+H=2OH$). The elementary reaction of consuming H, OH and O radicals at the high net reaction rate are consisted of R1 ($H+O_2=OH+O$), R2 ($H_2+O=OH+H$) and R3 ($H_2+OH=H_2O+H$).

ACKNOWLEDGMENTS

The authors appreciate the financial supported by National Natural Science Foundation of China (No. 51674059 and No. 51874066), Key Laboratory of Building Fire Protection Engineering and Technology of MPS (No. KFKT2016ZD01), Liaoning Provincial Natural Science Foundation of China (20170540160) and the Fundamental Research Funds for the Central Universities (DUT16RC(4)04).

REFERENCES

1. Kim, W.K., Mogi, T., Dobashi, R., Flame acceleration in unconfined hydrogen/air deflagrations using infrared photography, *Journal of Loss Prevention in the Process Industries*, 26, 2013, pp. 1501-1505.
2. Wu, F., Jomaas, G., Law, C.K., An experimental investigation on self-acceleration of cellular spherical flames, *Proceedings of the Combustion Institute*, 34, 2013, pp. 937-945.
3. Nishimura, I., Mogi, T., Dobashi, R., Simple method for predicting pressure behavior during gas explosions in confined spaces considering flame instabilities, *Journal of Loss Prevention in the Process Industries*, 26, 2013, pp. 351-354.
4. Azatyan, V.V., Shebeko, Y.N., Shebeko, A.Y., A numerical modelling of an influence of CH_4, N_2, CO_2 and steam on a laminar burning velocity of hydrogen in air, *Journal of Loss Prevention in the Process Industries*, 23, 2010, pp. 331-336.
5. Pang, L., Wang, C., Han, M., Xu, Z., A study on the characteristics of the deflagration of hydrogen-air mixture under the effect of a mesh aluminum alloy, *Journal of Hazardous Materials*, 299, 2015, pp. 174-180.
6. Cheikhravat, H., Goulier, J., Bentaib, A., Meynet, N., Chaumeix, N., Paillard, C.-E, Effect of water sprays on flame propagation in hydrogen/air steam mixtures, *Proceedings of the Combustion Institute*, 35, 2015, pp. 2715-2722.
7. Ingram, J.M., Averill, A.F., Battersby, P.N., Holborn, P.G., Nolan, P.F., Suppression of hydrogen-oxygen-nitrogen explosions by fine water mist: Part 1. Burning velocity, *International Journal of Hydrogen Energy*, 37, 2012, pp. 19250-19257.
8. Ingram, J.M., Averill, A.F., Battersby, P., Holborn, P.G., Nolan, P.F., Suppression of hydrogen/oxygen/nitrogen explosions by fine water mist containing sodium hydroxide additive, *International Journal of Hydrogen Energy*, 38, 2013, pp. 8002-8010.
9. Sikes, T., Mathieu, O., Kulatilaka, W.D., Mannan, M.S., Petersen, E.L., Laminar flame speeds of DEMP, DMMP, and TEP added to H_2- and CH_4-air mixture, *Proceedings of the Combustion Institute*, 37, 2019, pp. 3775-3781.
10. Li, Y., Bi, M., Li, B., Zhou, Y., Huang, L., Gao, W., Explosion hazard evaluation of renewable hydrogen/ammonia/air fuels, *Energy*, 159, 2018, pp. 252-263.
11. Li, Y., Bi, M., Li, B., Zhou, Y., Gao, W., Effects of hydrogen and initial pressure on flame characteristics and explosion pressure of methane/hydrogen fuels, *Fuel*, 233, 2018, pp. 269-282.
12. Li, Y., Bi, M., Zhang, S., Jiang, H., Gan, B., Gao, W., Dynamic couplings of hydrogen/air flame morphology and explosion pressure evolution in the spherical chamber, *International Journal of Hydrogen Energy*, 43, 2018, pp. 2503-2513.
13. Li, Y., Bi, M., Gao, W., Theoretical pressure prediction of confined hydrogen explosion considering flame instabilities, *Journal of Loss Prevention in the Process Industries*, 57, 2019, pp. 320-326.
14. Sun, Z., Liu, F., Bao, X., Liu, X., Research on cellular instabilities in outwardly propagating spherical hydrogen-air flames, *International Journal of Hydrogen Energy*, 37, 2012, pp. 7889-7899.
15. Gu, X., Li, Q., Huang, Z., Zhang, N., Measurement of laminar flame speeds and flame stability

analysis of tert-butanol-air mixtures at elevated pressures, *Energy Conversion and Management*, 52, 2011, pp. 3137-3146.
16. Xiao, H., He, X., Duan, Q., Luo, X., Sun, J., An investigation of premixed flame propagation in a closed combustion duct with a 90 °blend, *Applied Energy*, 134, 2014, pp. 248-256.
17. Kwon, O.C., Rozenehan, G., Law, C.K., Cellular instabilities and self-acceleration of outwardly propagating spherical flames. *Proceeding of the Combustion Institute*, 29, 2002, pp. 1775-1783.
18. http://web.eng.ucsd.edu/mae/groups/combustion/mechanism.html
19. Li, G., Zhou, M., Zhang, Z., Liang, J., Ding, H., Experimental and kinetic studies of the effect of CO_2 dilution on laminar premixed n-heptane/air flames. *Fuel*, 227, 2018, pp. 355-366.
20. Li, G., Huang, H., Kobayashi, N., He, Z., Osaka, Y., Zeng, T., Numerical study on effect of oxygen content in combustion air on ammonia combustion. *Energy*, 93, 2015, pp. 2053-2068.
21. Li, J., Huang, H., Kobayashi, N., Wang, C., Numerical study on laminar burning velocity and ignition delay time of ammonia flame with hydrogen addition. *Energy*, 126, 2017, pp. 796-809.